

Communication

# Solid-State NMR Characterization of the Structure of Self-Assembled Ile–Phe–OH

Izuru Kawamura <sup>1,2,\*</sup> , Hiroki Shirakata <sup>1</sup>, Yumi Ozawa <sup>2</sup>, Batsaikhan Mijiddorj <sup>2,3</sup>  and Kazuyoshi Ueda <sup>2</sup>

<sup>1</sup> Graduate School of Engineering Science, Yokohama National University, Yokohama 2408501, Japan; shirakata-hiroki-zy@ynu.jp

<sup>2</sup> Graduate School of Engineering, Yokohama National University, Yokohama 2408501, Japan; ozawa-yumi-nz@ynu.jp (Y.O.); batsaikhan-mijiddorj-tg@ynu.jp (B.M.); ueda-kazuyoshi-cz@ynu.ac.jp (K.U.)

<sup>3</sup> School of Engineering and Applied Sciences, National University of Mongolia, Ulaanbaatar 14201, Mongolia

\* Correspondence: izuruk@ynu.ac.jp; Tel.: +81-45-339-4224

Received: 28 April 2018; Accepted: 26 June 2018; Published: 29 June 2018



**Abstract:** Solid-state nuclear magnetic resonance (NMR) spectroscopy provides significant structural information regarding the conformation and dynamics of a variety of solid samples. In this study, we recorded the <sup>13</sup>C and <sup>15</sup>N solid-state NMR spectra of a self-assembled isoleucine-phenylalanine (Ile–Phe–OH) dipeptide. Immediately after the addition of hexane to a solution of concentrated peptide in ethyl acetate, the peptide visually aggregated into a nanofiber. Then, we obtained well-resolved <sup>13</sup>C and <sup>15</sup>N NMR signals of the natural, isotopic-abundant Ile–Phe–OH peptide in the nanofiber. Furthermore, we calculated the chemical shift values of the reported crystal structure of the Ile–Phe dipeptide via the density functional theory (DFT) calculation and compared these results with the experimental values. Notably, the two sets of values were in good agreement with each other, which indicated that the self-assembled structure closely reflected the crystal structure. Therefore, herein, we demonstrated that solid-state NMR characterization combined with DFT calculations is a powerful method for the investigation of molecular structures in self-assembled short peptides.

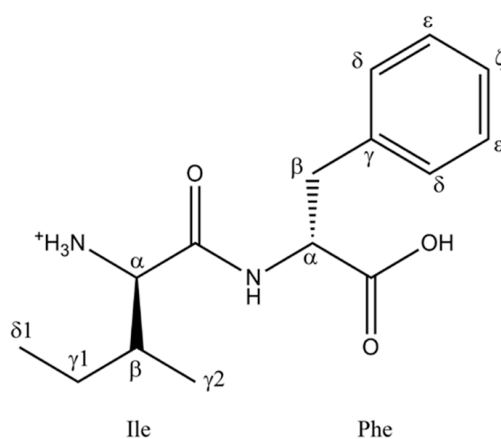
**Keywords:** solid-state NMR; dipeptide; self-assembly; natural isotopic abundance

## 1. Introduction

In supramolecular chemistry, the self-assembly of small molecules into highly ordered architectures has attracted significant interest. Many self-assembled systems are composed of a variety of weaker (non-covalent) interactions, such as hydrogen bonding and van der Waals forces, as well as electrostatic,  $\pi$ – $\pi$  stacking, and hydrophobic interactions [1]. For example, when diphenylalanine peptide (Phe–Phe–OH) is dissolved in 1,1,1,3,3,3-hexafluoro-2-isopropanol (HFIP) and water is added as a poor solvent, the peptide rapidly self-assembles into a nanofiber [2]. With respect to the dipeptide, hydrogen bonding and  $\pi$ – $\pi$  interactions among the inter-peptides play a crucial role in the growth of associated components [3]. Usually, studies on self-assembled dipeptides involve the use of HFIP as a first solvent, which dissolves the peptide at high concentrations, and the addition of water, which triggers the rapid self-association.

In this study, we prepared isoleucine-phenylalanine (Ile–Phe–OH) (Scheme 1) and subsequently dissolved it in ethyl acetate at high concentrations. Immediately after the addition of *n*-hexane to the formed solution, the peptide visually aggregated. Reportedly, for Phe–Phe–OH, different organic solvents can be used to control the self-assembly behavior and attain a solvent-dependent morphological change [4]. For instance, in aqueous or methanol solutions, Phe–Phe–OH self-assembles to form hollow tubular structures [4,5]. However, with the introduction of an acetonitrile–water solvent

to the mixture, a structural transition from diphenylalanine (Phe–Phe–OH) microtubes to highly uniform nanowires occurs [6]. These assembled structures are in fact considered useful for various applications [7,8], such as in piezoelectric devices and for cell membrane disruptions [9–11]. Therefore, it is important to characterize the molecular structure of self-assemblies in order to understand the functionalized peptide materials at the molecular level. To address this issue, our research group is presently investigating the molecular structures of several types of self-assembled peptides by solid-state nuclear magnetic resonance (NMR).



**Scheme 1.** The chemical structure of isoleucine-phenylalanine (Ile–Phe–OH).

Generally, solid-state NMR spectroscopy can provide structural insights not only on insoluble molecules, such as membrane proteins and amyloid fibers [12,13], but also on crystalline dipeptides [14,15]. Previously, the molecular structures of the self-assembled Phe–Phe–OH and cyclic dipeptides have been characterized by  $^{13}\text{C}$  solid-state NMR experiments [16,17]. Moreover, solid-state  $^{13}\text{C}$  and  $^{15}\text{N}$  NMR analyses have proved advantageous in the investigation of local dynamics, as well as the detection of structures containing –NH– hydrogen bonds and side-chain conformations in proteins and peptides [18–20]. Usually,  $^{13}\text{C}$  NMR chemical shift values of protein backbones and side chains are tightly coupled with secondary structures [18,19], while  $^{15}\text{N}$  NMR signals are sensitive, not only to conformations, but also to hydrogen bond strengths [21]. Based on these reports, solid-state NMR is considered useful in investigating the self-assembled molecular structure in the materials. Herein, we demonstrate the structural characterization of Ile–Phe–OH in nanofibers using solid-state NMR.

## 2. Results and Discussion

First, we observed the morphology of the Ile–Phe peptide as it self-assembled, formed after treatment with the ethyl acetate-hexane solution. Scanning electron microscope (SEM) images of the sample are shown in Figure 1. The morphology of the self-assembled peptide appeared as a straight fiber with an average width of around 80 nm, which was easily dissolved in an aqueous solution.

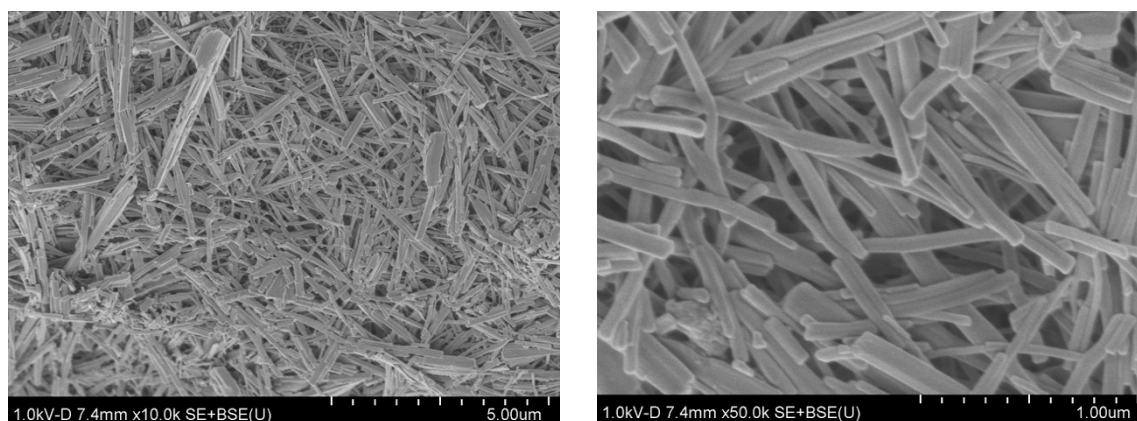


**Figure 1.** SEM images of the self-assembled fibers (scale bar: 5.00  $\mu\text{m}$ , left) and an expanded region of the image (scale bar: 1.00  $\mu\text{m}$ , right).

A  $^{13}\text{C}$  cross polarization-magic angle spinning (CP-MAS) NMR spectrum of Ile–Phe in the self-assembled state was obtained at 300 K, as shown in Figure 2. The spectrum displayed well-resolved, strong, and narrow isotropic peaks from all carbon atoms in the assembled Ile–Phe peptide, even though the peptide was synthesized with a natural abundance of isotopes. In addition, because the sample was sufficiently dried, the signals of n-hexane disappeared. Generally, the  $^{13}\text{C}$  NMR resonance positions of the individual amino acid residues in proteins are well-known and highly dependent on local secondary structures [19]. In addition, according to a  $^{13}\text{C}$  estimation using ChemBioDraw, all  $^{13}\text{C}$  NMR signals could be assigned to the resonances of the dipeptide (allocated  $^{13}\text{C}$  chemical shifts are summarized in Table 1). Additionally, the typical line-width of the  $^{13}\text{C}\gamma 1$  Ile1 signal at 25.8 ppm was 115.2 Hz, which indicates that the structural homogeneity of the peptide in the fiber was high. The isotropic  $^{13}\text{C}$  chemical shift of the backbone  $\text{C}\alpha$  and carbonyl carbons of the respective amino acid residues in model polypeptides are significantly displaced up to 6–8 ppm, depending on their local conformations [18,19]. The validity of the conformation-dependent  $^{13}\text{C}$  chemical shifts of particular residues from the simple model systems to more complicated proteins has been proven to be excellent and can be utilized as a diagnostic means to distinguish their local conformations, as far as in amyloid fibril, silk fiber, collagen, and transmembrane protein [22]. Thus, using conformation-dependent  $^{13}\text{C}$  chemical shift lists, the local secondary structure was readily identified. The signals of carbonyl  $^{13}\text{C}=\text{O}$  of Ile1,  $^{13}\text{C}\alpha$  of Ile1, and Phe2 appeared at 173.2, 57.1, and 52.3 ppm, respectively, and those resonances indicated the secondary structure of a  $\beta$ -sheet form [19,22]. The position of the carboxylic signal is very sensitive to the ionization state;  $\text{COO}^-$  is low-field resonance, and  $\text{COOH}$  is high-field resonance [23]. It is reported that carboxylic signal of the Phe–Phe–OH nanotube prepared by the addition of water appeared at around 180 ppm because of the forming ionization state ( $\text{COO}^-$ ) [17], while, the C-terminal carboxylic signal appeared at 167.2 ppm as  $\text{COOH}$ , which was an unusual resonance position. Furthermore, the resonance suggested that the C-terminal group might have a twisted conformation. Consequently, one defined angle  $\theta$  ( $\text{C}\beta 1\text{-C}\alpha 1\cdots\text{C}\alpha 2\text{-C}\beta 2$ ) might be close to  $0^\circ$ , which means the orientation of the side chains is on the same side of peptide bond plane [3]. Indeed, the backbone structure of Ile–Phe–OH in the crystal reportedly takes a twisted conformation at the C-terminal group ( $\theta = 16^\circ$ , see Table A1) [3]. In addition, usually, a  $^{13}\text{C}\delta 1$  Ile signal is related to the Ile side-chain orientation between the trans, gauche, and gauche (-) forms [24]. A signal position of  $^{13}\text{C}\delta 1$  Ile1 at 10.7 ppm shows the most populated trans conformation. It is suggested that the side-chain conformation contributes to intermolecular contact. Additionally, it is reported that, as opposed to Val–Phe–OH, self-assembled Ile–Phe–OH peptides form a strong gel in aqueous solutions [25]. However, according to our initial solvent screening, Ile–Phe–OH did not form a gel in an aqueous solution. We believe that the Ile side chain may play a key role in the formation of a highly ordered structure.

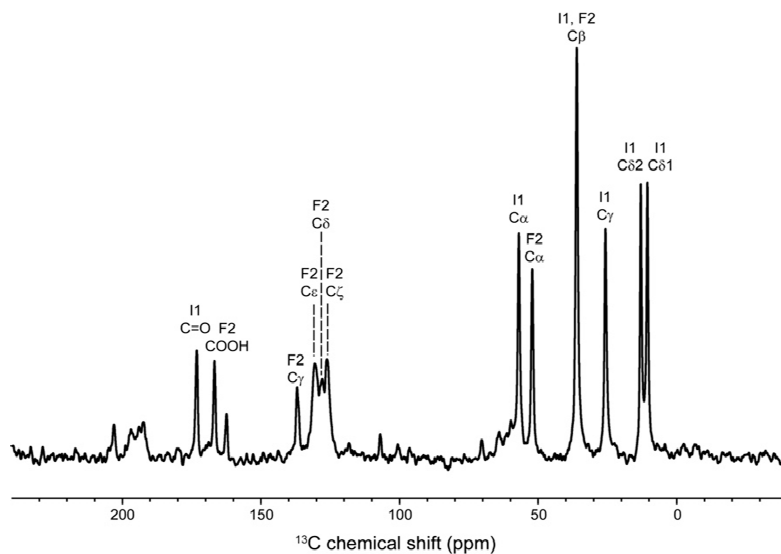


**Figure 2.**  $^{13}\text{C}$  cross polarization-magic angle spinning (CP-MAS) NMR spectrum of self-assembled Ile-Phe-OH after an ethyl acetate-hexane treatment. I1: Ile1; F2: Phe2; and ssb: spinning side band.

The  $^{15}\text{N}$  CP-MAS spectrum of self-assembled Ile-Phe-OH is shown in Figure 3. Two significant signals of N-terminal amine  $\text{NH}_3^+$  at Ile1 and amide  $-\text{NH}-$  at Phe2 appeared at 16.0 and 97.6 ppm, respectively, although the S/N ratio was rather low due to the extremely low  $^{15}\text{N}$  natural abundance (0.37%) and resonance frequency (60.81 MHz). Reportedly, the  $^{15}\text{N}$  chemical shifts of amides are dependent on the intermolecular hydrogen bond distance [14,21]. Hence, in the present study, the NMR signal of the amide indicates that the peptide formed an intermolecular hydrogen bond during the self-assembly process. Furthermore,  $^{15}\text{N}$  chemical shifts of amines are also affected by multiple hydrogen bonds [14]. Therefore, herein, the signal position at 16.0 ppm was identified with the formation of the hydrogen bond. Based on these results, we concluded that the role of hydrogen bonds in the formation of self-assembled structures is significant. Another contribution to consider is the steric effect on the amide nitrogen atom [26]. It is possible that such an effect could change the orientation of the Phe2 side chain, as well as twist the C-terminal group. As a result, the amide  $^{15}\text{N}$  signal appeared at less than 100 ppm.

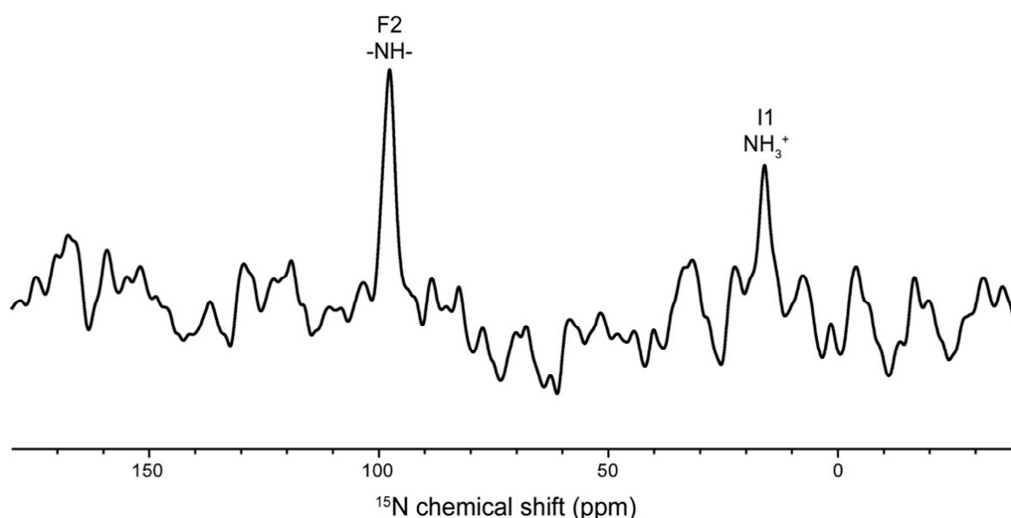


**Figure 3.**  $^{15}\text{N}$  CP-MAS NMR spectrum of self-assembled Ile-Phe-OH after an ethyl acetate-hexane treatment. I1: Ile1, and F2: Phe2.

The torsion angle likelihood obtained from shift (TALOS) system can predict the torsion phi and psi angles of protein backbone [27]. However, this system cannot be applied to dipeptides because the peptide is too short. Therefore, we performed quantum chemical calculations on the crystal structure and compared the obtained results to the experimental ones of the self-assembled structure. The crystal structure of the Ile–Phe dipeptide has been previously determined by Görbitz to contain two dipeptides and two water molecules in the unit cell [28,29]. Herein, we calculated the chemical shift values of the crystal structure using the density functional theory (DFT) calculation and compared the results with the experimental values of the synthesized self-assembled structure. The calculation was performed on the system using trimer dipeptide molecules extracted from the crystal structure (Figure A1), with the water molecules being deleted from the system. The results from the calculations and the experimental values of the self-assembled structure are summarized in Table 1. The chemical shifts of all carbon atoms, which exist inside the trimer structure (Figure A1), were in relatively good agreement with the experimental results, although those absolute values were not completely equal. The three torsion angles of peptide backbone in the crystal structure also showed that the C-terminal group takes twisted form and both side chains are located on the same side of peptide bond plane (Figure A1 and Table A1). On the other hand, a discrepancy was found in the N-terminal amine  $\text{NH}_3^+$  at Ile1 and C-terminal carbonyl carbon at Phe2 between the self-assembled and crystal structures. It is expected that this change was caused by the deletion of water molecules from the trimer model and the ionization state of  $\text{COO}^-$  in the crystal structure. Another discrepancy was also found in the atoms of  $\text{C}\gamma_2$  and  $\text{C}\delta_1$  at Ile1 and  $\text{C}\delta$ ,  $\text{C}\epsilon$ , and  $\text{C}\zeta$  at Phe2, which was probably caused by the lack of intermolecular side-chain interactions because of the existence of these atoms on the outside of the trimer structure from the crystal structure (Figure A1). Based on these results, we concluded that the intermolecular interactions of the trimer molecules represented well the interactions in the experimental structure. In addition, the obtained results indicate that the self-assembled structure should closely reflect the crystal structure. However, in order to further investigate the conformation of the self-assembled structure, more detailed calculations with several possible model structures would be needed. Nevertheless, the results from this study demonstrated that  $^{13}\text{C}$  and  $^{15}\text{N}$  solid-state NMR analysis combined with DFT calculations could potentially be an effective approach to investigate the local structure of self-assembled molecules.

**Table 1.**  $^{13}\text{C}$  and  $^{15}\text{N}$  NMR chemical shift values of self-assembled Ile–Phe after an ethyl acetate-hexane treatment and calculated values of the crystal structure of Ile–Phe–OH.

	Atom	Observed Chemical Shift (ppm)	Calculated Chemical Shift (ppm)
Ile1	$^{15}\text{NH}_3^+$	16.0	$3.2 \pm 1.3$
	$^{13}\text{C}\alpha$	57.1	$60.1 \pm 0.6$
	$^{13}\text{C}\beta$	36.2	$37.2 \pm 0.2$
	$^{13}\text{C}\gamma_1$	25.8	$23.3 \pm 0.1$
	$^{13}\text{C}\gamma_2$	13.0	$-0.3 \pm 0.3$
	$^{13}\text{C}\delta_1$	10.7	$-0.6 \pm 0.3$
	$^{13}\text{C}=\text{O}$	173.2	$150.1 \pm 0.4$
Phe2	$^{15}\text{NH}$	97.6	$97.9 \pm 2.5$
	$^{13}\text{C}\alpha$	52.3	$53.4 \pm 0.5$
	$^{13}\text{C}\beta$	36.2	$29.5 \pm 0.3$
	$^{13}\text{C}\gamma$	137.1	$141.7 \pm 1.8$
	$^{13}\text{C}\delta_1$	125.0	$115.9 \pm 0.6$
	$^{13}\text{C}\delta_2$		$121.9 \pm 0.6$
	$^{13}\text{C}\epsilon_1$	129.4	$121.2 \pm 0.4$
	$^{13}\text{C}\epsilon_2$		$116.6 \pm 0.4$
	$^{13}\text{C}\zeta$	127.5	$109.7 \pm 1.2$
$^{13}\text{COOH}$	167.2 (COOH)	$159.4 \pm 0.9 (\text{COO}^-)$	

### 3. Materials and Methods

Natural, isotopic-abundant Ile–Phe–OH was synthesized via a microwave-assisted solid-phase peptide method using an Initiator+ Alstra (Biotage) peptide synthesizer and was subsequently cleaved from the resin using 95% trifluoro-acetic acid (TFA) solution. The peptide was purified using a reverse-phase high-performance liquid chromatography (HPLC, Shimadzu Prominence system) system equipped with a Kinetex Axia C18 ODS column. The product (Ile–Phe–OH) was confirmed by its mass number,  $[M + H] = 279.01$   $m/z$ , using matrix-assisted laser desorption ionization time-of-flight mass spectrometry (MALDI-TOF-MS, Bruker Daltonics). The Ile–Phe–OH peptide was dissolved in ethyl acetate at a high concentration of 200 mg/mL. The formed solution was then diluted with *n*-hexane to a final peptide concentration of 10 mg/mL, after which the peptide rapidly self-assembled into an aggregate.

The morphology of the sample was identified by SEM (HITACHI High-Tech SU-8010). The nanofiber sample was dry, and 10 mg of the dried sample were packed into a 4.0 mm o.d. zirconia NMR rotor.  $^{13}\text{C}$  and  $^{15}\text{N}$  high-resolution solid-state NMR spectra were recorded on a Bruker Avance III (600 MHz) solid-state NMR spectrometer operating at 150.92 and 60.81 MHz for carbon and nitrogen nuclei, respectively, and equipped with a 4.0 mm E-free MAS probe. The number of scans was 5000 for  $^{13}\text{C}$  and 15,000 for  $^{15}\text{N}$ , and the probe temperature was set to 300 K. CP-MAS with a spinal 64 proton decoupling [30] was performed at a MAS frequency of 10.0 kHz. The  $^{13}\text{C}$  and  $^{15}\text{N}$  contact times were set to 1.0 and 2.0 ms, respectively. The  $^{13}\text{C}$  and  $^{15}\text{N}$  chemical shifts were externally referenced to 176.03 ppm for the carbonyl carbon of glycine (tetramethylsilane at 0.0 ppm) and 11.59 ppm for  $^{15}\text{NH}_4\text{NO}_3$ . The estimation of the  $^{13}\text{C}$  chemical shifts was performed using ChemBioDraw Ultra ver. 12.0.

For the DFT calculation, trimer dipeptide molecules were extracted from the crystal structure of Ile–Phe [28] and are shown in Figure A1. The system consisted of two dipeptide molecules in the unit cell and one additional neighbor dipeptide molecule. In the calculations, the water molecules were deleted from the unit cell, and the geometry of the system was not optimized to keep the arrangement of the molecules in the crystal structure. The chemical shift calculation was performed via the GIAO/DFT method using the B3LYP/6-31G\*\* basis set of the Gaussian 16 B.01 software [31].

### 4. Conclusions

Because short peptides can take various conformations, it is important to identify these in order to understand the mechanisms of peptide self-assembly. In this study, self-assembled Ile–Phe peptides obtained after an ethyl acetate-hexane treatment were obtained as nanofibers. Subsequently,  $^{13}\text{C}$  and  $^{15}\text{N}$  solid-state NMR measurements were performed on the self-assembled Ile–Phe peptide fibers, and the observed signals were also compared with the calculated ones from the crystal structure. The observed chemical shift values are generally consistent with the calculated values, although a few discrepancies remain. Accordingly, we found that the structure of the self-assembled Ile–Phe peptide was very similar with the crystal structure. We also demonstrated that solid-state NMR structural analysis combined with DFT calculations of self-assembled dipeptides is an effective approach.

**Author Contributions:** I.K., H.S., and Y.O. conceived of and designed the experiments; H.S. and Y.O. performed the experiments; B.M. and K.U. performed the DFT calculations; I.K., H.S., and Y.O. analyzed the data; and I.K. wrote the paper.

**Funding:** This work was partly supported by the Grants-in-Aid for Scientific Research from the Ministry of Culture, Sports, Science, and Technology of Japan (JSPS KAKENHI) to I. K. (16H00828 and 18H02387).

**Acknowledgments:** The authors thank Shinji Ishihara at the Instrumental Analysis Center of Yokohama National University for his technical assistance with the optimization of the NMR spectrometer and probe performance. DFT calculations were performed by the Research Center for Computational Science, Okazaki, Japan. B. M. was granted a scholarship by the Mongolian-Japan Engineering Education Development Program (J11B16).

**Conflicts of Interest:** The authors declare no conflict of interest.

## Appendix A

The trimer dipeptide molecules were extracted from the crystal structure of the Ile–Phe dipeptide, which was determined by Görbitz [28]. The trimer structure was shown in Figure A1 and used for the chemical shift calculation. The structure visualization and dihedral angle calculations were performed by VMD software [32].

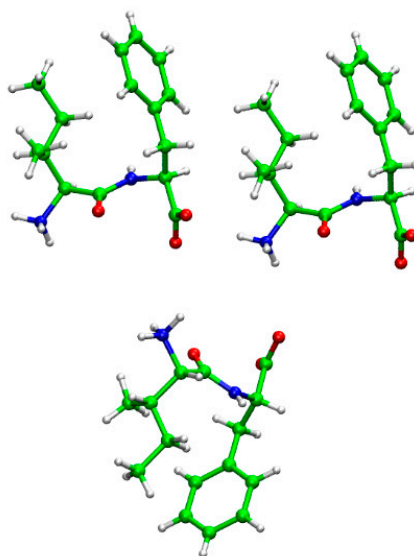


**Figure A1.** The trimer structure that is used in the chemical shift calculation.

**Table A1.** The dihedral angles in the main chain of the crystal structure.

Angle Names	Angles (degrees)
$\phi$ (C'1-N2- C $\alpha$ 2-C'2)	49.49
$\varphi$ (N1- C $\alpha$ 1-C1'-N2)	149.92
$\omega$ (C $\alpha$ 1-C'1-N2- C $\alpha$ 2)	170.64
$\theta$ (C $\beta$ 1-C $\alpha$ 1...C $\alpha$ 2- C $\beta$ 2)	16.02

## References

- Shimizu, T.; Minamikawa, H.; Kogiso, M.; Aoyagi, M.; Kameta, N.; Ding, W.; Masuda, M. Self-organized nanotube materials and their application in bioengineering. *Polym. J.* **2014**, *46*, 831–858. [[CrossRef](#)]
- Reches, M.; Gazit, E. Casting metal nanowires within discrete self-assembled peptide nanotubes. *Science* **2003**, *300*, 625–627. [[CrossRef](#)] [[PubMed](#)]
- Görbitz, C.H. Microporous organic materials from hydrophobic dipeptides. *Chem. Eur. J.* **2007**, *13*, 1022–1031. [[CrossRef](#)] [[PubMed](#)]
- Mason, T.O.; Chirgadze, D.Y.; Levin, A.; Adler-Abramovich, L.; Gazit, E.; Knowles, T.P.J.; Buell, A.K. Expanding the solvent chemical space for self-assembly of dipeptide nanostructures. *ACS Nano* **2014**, *8*, 1243–1253. [[CrossRef](#)] [[PubMed](#)]
- Görbitz, C.H. The structure of nanotubes formed by diphenylalanine, the core recognition motif of Alzheimer's  $\beta$ -amyloid polypeptide. *Chem. Commun.* **2006**, 2332–2334. [[CrossRef](#)] [[PubMed](#)]
- Huang, R.; Wang, Y.; Qi, W.; Su, R.; He, Z. Temperature-induced reversible self-assembly of diphenylalanine peptide and the structural transition from organogel to crystalline nanowire. *Nanoscale Res. Lett.* **2014**, *9*, 653. [[CrossRef](#)] [[PubMed](#)]
- Adler-Abramovich, L.; Gazit, E. The physical properties of supramolecular peptide assemblies: From building block association to technological applications. *Chem. Soc. Rev.* **2014**, *43*, 6881–6893. [[CrossRef](#)] [[PubMed](#)]
- Yan, X.; Zhu, P.; Li, J. Self-assembly and application of diphenylalanine-based nanostructures. *Chem. Soc. Rev.* **2010**, *39*, 1877–1890. [[CrossRef](#)] [[PubMed](#)]

9. Nguyen, V.; Zhu, R.; Jenkins, K.; Yang, R. Self-assembly of diphenylalanine peptide with controlled polarization for power generation. *Nat. Commun.* **2016**, *7*, 13566. [[CrossRef](#)] [[PubMed](#)]
10. Jeena, M.T.; Palanikumar, L.; Go, E.M.; Kim, I.; Kang, M.G.; Lee, S.; Park, S.; Choi, H.; Kim, C.; Jin, S.-M.; et al. Mitochondria localization induced self-assembly of peptide amphiphiles for cellular dysfunction. *Nat. Commun.* **2017**, *8*, 26. [[CrossRef](#)] [[PubMed](#)]
11. Schnaider, L.; Brahmachari, S.; Schmidt, N.W.; Mensa, B.; Shaham-Niv, S.; Bychenko, D.; Adler-Abramovich, L.; Shimon, L.J.W.; Kolusheva, S.; DeGrado, W.F.; et al. Self-assembling dipeptide antibacterial nanostructures with membrane disrupting activity. *Nat. Commun.* **2017**, *8*, 1365. [[CrossRef](#)] [[PubMed](#)]
12. Naito, A.; Kawamura, I.; Javkhlantugs, N. Recent solid-state NMR studies of membrane bound peptides and proteins. In *Annual Reports of NMR Spectroscopy*; Webb, G.A., Ed.; Elsevier: New York, NY, USA, 2015; Volume 86, pp. 333–411. [[CrossRef](#)]
13. Naito, A.; Kawamura, I. Solid-state NMR as a method to reveal structure and membrane-interaction of amyloidogenic proteins and peptides. *Biochim. Biophys. Acta Biomembr.* **2007**, *1768*, 1900–1912. [[CrossRef](#)] [[PubMed](#)]
14. Altheimer, B.D.; Mehta, A.M. Effects of structural differences on the NMR chemical shifts in isostructural dipeptides. *J. Phys. Chem. A* **2014**, *118*, 2618–2628. [[CrossRef](#)] [[PubMed](#)]
15. Bhate, M.P.; Woodard, J.C.; Mehta, M.A. Solvation and hydrogen bonding in alanine- and glycine-containing dipeptides probed using solution- and solid-state NMR spectroscopy. *J. Am. Chem. Soc.* **2009**, *131*, 9579–9589. [[CrossRef](#)] [[PubMed](#)]
16. Jeziorna, A.; Stopczyk, K.; Shorupska, E.; Luberda-Durnas, K.; Oszejca, M.; Lasocha, W.; Górecki, M.; Frelek, J.; Potrzebowski, M.J. Cyclic dipeptides as building units of nano- and microdevices: Synthesis, properties, and structural studies. *Cryst. Growth Des.* **2015**, *15*, 5138–5148. [[CrossRef](#)]
17. Jaworska, M.; Jeziorna, A.; Drabik, E.; Potrzebowski, M.J. Solid state NMR study of thermal processes in nanoassemblies formed by dipeptides. *J. Phys. Chem. C* **2012**, *116*, 12330–12338. [[CrossRef](#)]
18. Saitô, H. Conformation-dependent  $^{13}\text{C}$  chemical shift: A new means of conformational characterization as obtained by high-resolution solid-state  $^{13}\text{C}$  NMR. *Magn. Reson. Chem.* **1986**, *24*, 835–852. [[CrossRef](#)]
19. Saitô, H.; Ando, I.; Ramamoorthy, A. Chemical shift tensor—the heart of NMR: Insight into biological aspects of proteins. *Prog. Nucl. Magn. Reson. Spectrosc.* **2010**, *57*, 181–228. [[CrossRef](#)] [[PubMed](#)]
20. Kawamura, I.; Ohmine, M.; Tanabe, J.; Tuzi, S.; Saitô, H.; Naito, A. Dynamic aspects of extracellular loop region as a proton release pathway of bacteriorhodopsin studied by relaxation time measurements by solid state NMR. *Biochim. Biophys. Acta biomembr.* **2007**, *1768*, 3090–3097. [[CrossRef](#)] [[PubMed](#)]
21. Kuroki, S.; Asakawa, N.; Ando, S.; Ando, I.; Shoji, A.; Ozaki, T. Hydrogen bond length and  $^{15}\text{N}$  NMR chemical shift of the glycine residue of some oligopeptide in the solid state. *J. Mol. Struct.* **1991**, *245*, 69–80. [[CrossRef](#)]
22. Saitô, H.; Naito, A. NMR studies on fully hydrated membrane proteins, with emphasis on bacteriorhodopsin as a typical and prototype membrane protein. *Biochim. Biophys. Acta* **2007**, *1768*, 3145–3161. [[CrossRef](#)] [[PubMed](#)]
23. Metz, G.; Siebert, F.; Engelhard, M. High-resolution solid state  $^{13}\text{C}$  NMR of bacteriorhodopsin: Characterization of  $[4-^{13}\text{C}]$ asp resonances. *Biochemistry* **1992**, *31*, 455–462. [[CrossRef](#)] [[PubMed](#)]
24. Hansen, D.F.; Neudecker, P.; Kay, L.E. Determination of isoleucine side-chain conformations in ground and excited states of proteins from chemical shifts. *J. Am. Chem. Soc.* **2010**, *132*, 7589–7591. [[CrossRef](#)] [[PubMed](#)]
25. de Groot, N.S.; Parella, T.; Aviles, F.X.; Vendrell, J.; Ventura, S. Ile-phe dipeptide self-assembly: Clues to amyloid formation. *Biophys. J.* **2007**, *92*, 1732–1741. [[CrossRef](#)] [[PubMed](#)]
26. Le, H.; Oldfield, E. Correlation between  $^{15}\text{N}$  NMR chemical shifts in proteins and secondary structure. *J. Biomol. NMR* **1994**, *4*, 341–348. [[CrossRef](#)] [[PubMed](#)]
27. Shen, Y.; Delaglio, F.; Cornilescu, G.; Bax, A. TALOS+: A hybrid method for predicting protein backbone torsion angles from NMR chemical shifts. *J. Biomol. NMR* **2009**, *44*, 213–223. [[CrossRef](#)] [[PubMed](#)]
28. Görbitz, C.H. L-isoleucyl-L-phenylalanine dihydrate. *Acta Crystallogr. Sect. C* **2004**, *60*, o371–o373. [[CrossRef](#)] [[PubMed](#)]

29. Görbitz, C.H. Nanotube formation by hydrophobic dipeptides. *Chem. Eur. J.* **2001**, *7*, 5153–5159. [[CrossRef](#)]
30. Fung, B.M.; Khitritin, A.K.; Ermolaev, K. An improved broadband decoupling sequence for liquid crystals and solids. *J. Magn. Reson.* **2000**, *142*, 97–101. [[CrossRef](#)] [[PubMed](#)]
31. Frisch, M.J.; Trucks, G.W.; Schlegel, H.B.; Scuseria, G.E.; Robb, M.A.; Cheeseman, J.R.; Scalmani, G.; Barone, V.; Petersson, G.A.; Nakatsuji, H.; et al. *Gaussian 16 Rev. B.01*; Gaussian, Inc.: Wallingford, CT, USA, 2016.
32. Humphrey, W.; Dalke, A.; Schulten, K. VMD: Visual Molecular Dynamics. *J. Mol. Graph.* **1996**, *14*, 33–38. [[CrossRef](#)]



© 2018 by the authors. Licensee MDPI, Basel, Switzerland. This article is an open access article distributed under the terms and conditions of the Creative Commons Attribution (CC BY) license (<http://creativecommons.org/licenses/by/4.0/>).